Bezazi, A., Boumediri, H., Del Pino, G. G., Bezzazi, B., Scarpa, F. L., Reis, P. N. B., & Dufresne, A. (Accepted/In press). Alkali treatment effect on physicochemical and tensile properties of date palm rachis fibers. *Journal of Natural Fibers*.

Alkali treatment effect on physicochemical and tensile properties of date palm rachis fibers

Abderrezak Bezazi[a], Haithem Boumediri[a], Gilberto Garcia Del Pino[b], Boudjema Bezzazi[c], Fabrizio Scarpa[d], Paulo N.B. Reis[e], Alain Dufresne[f]*

[a]*Laboratoire de Mécanique Appliquée des Nouveaux Matériaux (LMANM), Université 8 Mai 1945, Guelma, Algeria.*

[b]*Department of Mechanical Engineering, State University of Amazonas, Manaus-AM/Brazil, Brazil.*

[c]*Research Unit Materials, Processes and Environment (RU-MPE), University M'Hamed Bougara, Boumerdes 35000, Algeria.*

[d]*Department of Aerospace Engineering, University of Bristol, Queens Building, University Walk BS8 1TR Bristol, UK.*

[e]*C-MAST, Depart. of Electromechanical Engineering, University of Beira Interior, 6201-001 Covilhã, Portugal.*
[f]*Univ. Grenoble Alpes, CNRS, Grenoble INP, LGP2, F-38000, France.*

*Corresponding author: alain.dufresne@pagora.grenoble-inp.fr

ORCID:

Abderrezak Bezazi	https://orcid.org/0000-0002-4461-6689
Haithem Boumediri	https://orcid.org/0000-0002-9578-0948
Gilberto Garcia Del Pino	https://orcid.org/0000-0003-0754-2390
Fabrizio Scarpa	https://orcid.org/0000-0002-5470-4834
Paulo N.B. Reis	http://orcid.org/0000-0001-5203-3670
Alain Dufresne	https://orcid.org/0000-0001-8181-1849

Alkali treatment effect on physicochemical and tensile properties of date palm rachis fibers

ABSTRACT: This work aims to optimize the physico-chemical and tensile properties of vascular fibers extracted from a local date palm rachis in Algeria. This fiber has a very specific composition and architecture and is different from the remaining fibers obtained from the six possible parts of the tree. For this purpose, a Taguchi orthogonal array design L16 was applied to reduce the number of experiments. The fibers were extracted from the rachis with two different methods (boiling and retting in water) and treated by NaOH with various concentrations (1%, 2%, 3%, and 5%) and for different durations (1, 4, 8 and 12 hours). They were characterized using SEM-EDX, ATR-FTIR, XRD and TGA to understand the effects of the extraction method and alkali treatment. A statistical treatment of the data was carried out based on the S/N ratio and ANOVA was performed to identify the most significant parameters affecting the tensile strength and the Young's modulus of the fibers. A desirability function was developed to identify the optimal factors leading to the maximization of the tensile properties.

Keywords: Date palm fibers, Vascular bundles, Alkali treatment, Taguchi design, Tensile and physicochemical properties.

1. INTRODUCTION

Currently, natural fibers obtained directly from plants (lignocellulosic) prove to be a viable solution to replace synthetic fibers. They are biodegradable ecological materials extracted from renewable resources and feature relatively low production costs (Bezazi et al. 2014; Siakeng et al. 2019). Natural fibers are also easily available in fibrous form with high specific properties and good thermal and acoustic insulation compared to many synthetic fibers (Fatma et al. 2019; Prabhakaran et al. 2020). Apart from the environmental impacts and practical advantages of lignocellulosic fibers, there are other reasons for the production or extraction of this type of reinforcements, such as their contribution to meeting the social, economic, and material needs of producers in some countries (Al-Oqla et al. 2015; Saba et al. 2017). Lignocellulosic fibers are also considered as one of the most important natural fibers used in various industrial sectors, and they come from many different sources such as wood, plants, and agro-waste (El-abbassi et al. 2020; Sanjay et al. 2019).

Agricultural residues and wastes are an important source of biomaterials for many industrial applications. In this context, a significant number of researchers are developing studies to use and valorize these agricultural by-products. Recent work related to those activities has been focusing on the use of natural fibers as reinforcement in biocomposites such as corn stalks, soy stalks and wheat straw (Nagarajan, Mohanty, and Misra 2013), coir pith, rice husk and groundnut shell (Prithivirajan et al. 2016), oil palm fiber (Sukudom et al. 2019), hemp (Assarar et al. 2016), jute (Toubal et al. 2018) and flax fiber (Cheour et al. 2016). However, according to several studies, the geographical origin of the plant and the method of extracting the fibers strongly influence their mechanical properties as well as their interaction with the matrix (KılınÇ et al. 2018; Mumthas, Wickramasinghe, and Gunasekera 2019). To overcome these disadvantages, literature suggests different chemical treatments like alkalization, silane treatment, benzoylation, acetylation, sodium chlorite, oleoyl chloride, permanganate, peroxide, triazine and stearic acid (Adekomaya and Majozi 2019; Gholampour and Ozbakkaloglu 2020; Sanjay et al. 2019). Different studies have been carried out to identify the best combination of chemical treatment parameters, as well as to understand the effect of each of them with a minimal number of experiments using different experimental design methods. Examples of these techniques involve the use of response surface methodology, Taguchi methods, Box-Behnken design, full-factorial design, fractional factorial design, Plackett-Burman design, D-optimal designs and Central Composite Design (Gündoıdu et al. 2016).

Date palm belongs to the *Phoenix dactylifera* L. family, and it is considered as an important fruit tree in Algeria with more than 20 million palm trees (Boumediri et al. 2019). This large number of trees makes Algeria the largest country in Africa and the world's fourth largest producer of dates, with approximately 1.1 million tons and an increase of over 98% between 2008 and 2018 (Food and Agriculture Organization 2018) (Anon n.d.). In addition, there are around 1,000 types of Algerian palms, including soft, dry and semi-dry varieties, each adapting to different types of soil and weather conditions (Laghouiter et al. 2018). However, as shown in Figure 1, date palm tree is constituted by six different parts (rachis, leaflets, petiole, fruit branches, mesh and trunk) and each part is composed by fibers with different composition and architecture. Therefore, all these different parts produce a significant amount of waste, totaling more than 800,000 tons per year in Algeria alone (Agoudjil et al. 2011; Amroune et al. 2019).

Figure 1

Considering these numbers and the current interest in bio-resources, literature reports several studies in which the fibers obtained in these different parts of the date palm are used as reinforcement for composite materials. Amroune et al. (Amroune et al. 2015), for example, extracted the fiber from the date palm fruit branches and studied the effect of alkali treatment on the mechanical and chemical properties. These authors observed that the alkali treatment increases the tensile strength and Young's modulus by 178% and 167%, respectively. Simultaneously, the treatment reduces the number of O-H links which decrease the hydrophilic nature of the fibers and improve their interaction with the matrix. On the other hand, the fibers obtained from date palm leaflets were investigated by Mohanty et al. (Mohanty et al. 2014) and, compared to untreated fibers, an increase of more than 116% and 25% was observed in terms of tensile strength and crystallinity index, respectively, after exposure to treatment with acrylic acid. Abdal-hay et al. (Abdal-Hay et al. 2012) investigated the effect of diameter and alkali treatment on the tensile properties of date palm fiber mesh. In terms of fiber diameter, lower values have a greater effect on the tensile properties of composites than coarse fibers. On the other hand, compared to raw fiber, they observed that the fibers treated with NaOH increased the tensile strength about 57%.

Modern techniques of retting including water retting were developed such as:

- Water retting with warm instead of cold water, which reduces the time between 70 and 100 hours of the process under controlled conditions (temperature and pH) (Konczewicz et al. 2013).
- Water retting with chemical activators or additives such as urea, sulfate, ammonium oxalate, sodium oxalate, calcium, and magnesium phosphate may be added to enhance the process by creating a highly nutritious environment for the growth and activity of the retting microbial community. However, this method results in very high water consumption and considerable effluent production (Das et al. 2014; Konczewicz et al. 2013).
- Water retting with a chemical solution, which is typically performed using a sodium hydroxide solution (NaOH) under controlled conditions leading to accelerated process of water retting but only for a few hours. This method is usually expensive and the need for the purchasing of special devices to run the process, water consuming, so it is not widely used (Konczewicz et al. 2013; Pandey 2007).

- Water retting with the presence of enzymes such as Endopolygalacturonase, pectinases, hemicellulases and cellulases that can replace bacteria and lead to facilitate fermentation and accelerate the production process (Akin et al. 2002; Liu et al. 2016).

However, according to the authors' knowledge, literature does not report studies on rachis fibers obtained from Ghars date palm trees (Fig. 1). The Ghars date palm used in this study represents more than 10% of the total date trees in Algeria, producing more than 20,000 tons of fronds waste (Boumediri et al. 2019). Therefore, in this socioeconomic context, the present work intends to optimize the tensile properties of Algerian date palm rachis fibers in order to be used as bio-reinforcement for composite materials. These fibers were extracted from the date palm rachis using two methods, the first with retting in water for three weeks and the second with boiling in water for 2.5 hours. Finally, the Taguchi method was used to optimize the tensile properties of this fiber treated with different NaOH concentrations and immersion times, as well as their physicochemical properties. The tensile properties were analyzed by ANOVA to understand the effect of each variable on the tensile strength and Young's modulus. Additional techniques like environmental scanning electron microscopy (ESEM) and energy-dispersive X-ray spectroscopy (EDX) were used to characterize the surface morphology and to determine the atomic percentage of present elements, respectively. The changes in functional groups on fiber surface after alkali treatment were determined using attenuated total reflectance Fourier transform infrared spectroscopy (ATR-FTIR), the fibers crystallinity was investigated by X-ray diffraction (XRD) and the thermal behaviour as well as the degradation of the main components of the fibers were determined using thermogravimetric analysis (TGA).

2. MATERIALS AND METHODS

2.1. Materials

A large number of date palm varieties exist; around 1,000 types of Algerian palms are currently listed including soft, dry and semi-dry varieties such as Deglet Nour, Degla Beida, Ghars, Mech Degla, Tafezouine and Fergus. An analysis of the production of each tree by category shows that the Ghars palm variety represents up to 10% of the total production in Algeria (Boumediri et al. 2019). Due to their abundance, Ghars palm leaves from El-Oued (South-Eastern Algeria) were used. The rachis taken from the palm tree was obtained by removing the leaflets and it was cut into uniform size about 8

inches in length using a drywall saw. The fibers were extracted from the rachis by two methods: the first with retting in water for three weeks and the second into boiling water for 2.5 hours. The bark with the cortex of the date palm rachis was then degummed to facilitate the extraction process and then the fibers were separated individually from the gums, waxes, and pectin. Ten Ghars date palm rachis were used in this work and each one yielded approximately 300 fibers for both extraction methods, which represents approximately 40% to 45% of the rachis weight. The separated vascular fibers were thoroughly washed with water and then air-dried for 8 hours and kept in a vacuum oven for 5 hours at 80°C to remove the moisture.

2.2. Design of experiments process

The Taguchi Method or sometimes called the Robust Design Method has been developed since the 1950s by Genichi Taguchi to assess and implement improvements in desired responses and at the same time simultaneously reduce the number of defects by studying the controlling factors and their levels to get the best results with a minimum number of experiences. This method has been widely used in several fields: materials, process and equipment to improve desired responses.

In this study, three factors that influence the tensile strength (TS) and Young's modulus (E) were considered. The parameters and their various levels are shown in Table 1. A total of 16 experiments and combinations of variables are derived from Taguchi's orthogonal array L16 (4^2 x 2^1) as shown in Table 2.

Table 1 **Table 2**

The alkaline treatment process was carried out in a similar manner to the work of previous authors (Amroune et al. 2015, 2019). Twenty fiber specimens were tested for each trial, i.e. a total of 360 tensile tests (40 for untreated fibers and 320 for treated fibers). In order to maximize TS and E, they were used as output measures in the Taguchi design analysis to determine the optimal configuration. The experimental data were transformed into a signal-to-noise ratio (S/N) for the analysis where it is assumed that the larger the better (LB) and can be calculated as a logarithmic transformation of the loss function by using the following equation:

$$\eta = -10\log_{10}\left[\frac{1}{n}\sum_{i=1}^{n}\frac{1}{Y_i^2}\right] \qquad (1)$$

Where η is the signal-to-noise ratio (dB), *n* is the number of observations under the same experimental conditions, and *Y* is the response value obtained in the test (output). ANOVA analyses were then performed to determine the distinctive factors influencing TS and E. Then, regression analysis was used to construct the mathematical equations for TS and E versus the independent variables to create a regression model. Besides, the optimum parameter levels were determined by the desirability function to get simultaneous maximization of TS and E.

2.3. Experimental procedure

2.3.1 Tensile tests

Twenty specimens from each group were tested at room temperature under tensile loading with a gauge length of 30 mm and a crosshead speed of 1 mm/min according to ASTM D3822-07 using a Zwick/Roell model Z2.5 Universal Testing Machine equipped with a load cell of 200 N. The tensile strength and Young's modulus were calculated individually for each fiber and the average values of each group of the twenty fibers are summarized in Table 2. The Young's modulus was obtained from the slope of the elastic part of the stress/strain curves between the strain values of 0.3 and 0.9%. The average diameter of the fibers was measured at three different zones along the fibers before the tensile tests with a Motic-BA310 Met optical microscope (Table 2).

2.3.2. Scanning electron microscopy (SEM)

The morphology of untreated and alkali-treated vascular date palm rachis fibers was investigated by SEM using a Quanta 200-FEI environmental SEM with Everhart-Thornley (ETD) secondary electron detector under low vacuum mode at a pressure of 0.3 Torr, operated at an acceleration voltage of 10 kV and at a working distance of about 10 mm. The fiber surfaces were analyzed using energy-dispersive X-ray spectroscopy (SEM-EDX) to determine the atomic percentage of present elements.

2.3.3. Fourier transform infrared spectrometry (FTIR)

The changes in functional groups on the fiber surface after alkali treatment were determined by FTIR spectra recorded on an ATR-FTIR using a Thermo Scientific model Nicolet iS10 FT-IR spectrometer equipped with Smart ATR accessory. The FTIR

spectral analysis was recorded in the range of 4000-500 cm^{-1} region with 32 scans at a resolution of 1 cm^{-1}.

2.3.4. X-ray powder diffraction (XRD)

XRD patterns for raw and treated fibers were collected using a Panalytical X'Pert-PRO, model: PW3050/60 diffractometer with a PW3064 sample spinner and X'Celerator Detector with an active length of 1.922° active length. The generator settings were 40mA/45kV with CuKα radiation of λ = 1.54059Å and the samples were scanned in the 2θ range of 6–60° at a speed of 0.02°/s. The crystallinity index (Cr.I.), the degree of crystallinity (Xc%) and the crystallite size (CS) were determined in the same way as for similar investigations (Boumediri et al. 2019; Das et al. 2018; Suryanto et al. 2014).

2.3.5. Thermogravimetric analysis (TGA)

Thermal stability of the fibers was assessed using a thermogravimetric analyzer (METTLER TOLEDO) with samples of approximately 10 mg at a rate 10 °C/min heated from 30°C to 700°C, carried out in N_2 atmosphere with a constant gas flow rate of 30 mL/min.

3. RESULTS AND DISCUSSION

3.1 Tensile tests analysis

The tensile strength (TS) value for the untreated fibers extracted by boiling (UEB) and retting in water (UER) was found to be 116.06 ±32.69 and 103.63 ±24.87 MPa, respectively, and their E (Young's modulus) value was 5.64 ±1.94 and 4.38 ±1.14 GPa, respectively (Table 2). The UEB fibers appear to provide improved tensile properties compared to UER fibers, and this is in good agreement with analogous data from the literature (Chonsakorn, Srivorradatpaisan, and Mongkholrattanasit 2019). From the typical stress-strain curves (Figure 2), it can be observed that the behaviour is nonlinear until the rupture of the fibers and this non-linearity is more pronounced for the treated fibers. The highest TS value obtained was 227.04 ±95.24 MPa recorded for the fibers extracted by boiling and treated with 3% NaOH for 8h of immersion (TEB3N8h) which is more than 95% higher that the value obtained for the untreated samples. However, the highest E value of 8.66 ±2.66 GPa was observed for the TEB3N12h reinforcement. Whilst the highest TS and E values for the fibers extracted by retting in water were

found to be 192.70 ± 46.58 MPa and 7.89 ± 1.42 GPa, respectively, at 3% for TEB3N4h, corresponding to an increase of about 86% for TS and 97% E compared to untreated fibers. Furthermore, the increase of NaOH concentration and immersion time leads to a decrease in TS and E of the fibers for both extraction methods.

Figure 2 **Table 3**

Table 3 shows the ANOVA analysis used to statistically treat the Taguchi results and investigate the significance of the effect of each parameter using P-values. At the same time, the significance of each term of the model was assessed using F-values. P-values lower than 0.05 imply statistical significance, while high F-values indicate that the selected empirical models are also significant. The highest F-value was found for the immersion time factor for the TS and E responses indicating its greater influence compared to others which can also be noticed in the main effect plot for Means and S/N ratio (Figure 3). From the analysis of the P-values it can be noticed that all parameters are significant in the case of TS. In the case of the Young's modulus the immersion time was the only significant parameter, but the extraction method was weakly significant and the NaOH concentration was not significant. ANOVA has shown that the model was significant for both responses. A nonlinear quadratic regression was developed for the response of TS and E in terms of coded factors that can be given by the following equations:

$$TS = 164.51 + 27.86A + 12.54B - 41.82C - 6.66A^2 - 0.54B^2 - 0.29AB + 10.14AC - 1.22BC \quad (2)$$

$$E = 5.552 + 0.209A + 0.648B - 0.451C - 0.182A^2 - 0.014B^2 - 0.019AB + 0.605AC - 0.186BC \quad (3)$$

Experimental values were compared with the predicted values, and Figure 4 evidences the good accuracy of the model (R^2 higher than 95%).

Figure 3 **Figure 4**

In order to optimize the TS and E values simultaneously, the desirability function was adopted and the 3D response surface, as well as 2D contour plots are shown in Figure 5. The response prediction desirability was found to be 94.36%, which gives a TS of 225.07 ±4.88 MPa and E of 8.977 ±0.24 GPa for the fibers extracted by boiling method and treated with 2.24% of NaOH for 11h 38 min immersion time.

Figure 5

3.2. Morphological analysis

SEM observation provides an excellent way to understand the effect of the extraction method and the alkali-treatment conditions on the fiber surface. Therefore, Figure 6a-b shows that the surface for UEB and UER fibers is covered with hemicelluloses, lignin, pectin, waxy substances, and other organic materials, whose presence is mainly due to the extraction method. However, when the fibers are exposed to alkali treatment (Figure 6c-d) non-cellulosic materials and impurities are eliminated, and additionally pores appear on the surface without any visible damage. Nevertheless, it is notice that UEB fibers are cleaner and have more pores than UER fibers. Finally, Figure 6e-f shows the longitudinal section of a treated fiber for different magnifications (×800 and ×3000, respectively). It is possible to observe a parallel set of interconnected microfibrils and several spherical bodies with a spiky shape known as silica bodies, which are found in scattered elliptical cavities on their surface. The alkali treatments not only resulted in changes in the mechanical properties of the treated fibers, but they also affected their surface structure (García Del Pino et al. 2020; Hanana et al. 2015; Sajid et al. 2019).

Figure 6

SEM-EDX analysis of the outer surface of the UEB and TEB3N8h fibers indicated remarkable changes in the elemental content as well as in their morphology (Figure 7). The fibers basically consist of carbon (C), oxygen (O) elements, as well as other elements in small amounts, like sodium (Na), aluminum (Al), silica (Si), chlorine (Cl), potassium (K), calcium (Ca) and sulfur (S). In general, the surface behaviour of the different lignocellulosic fibers is compared to the theoretical atomic ratio between oxygen to carbon (O/C ratio), which is 0.83 for pure cellulose, 0.33 for lignin and the lowest ratio is 0.1 for extractives (Ma et al. 2016). The O/C ratio measured for untreated and treated fibers is 0.68 and 0.78, respectively. This proves the effectiveness of the alkaline treatment to remove impurities, leading to an increase in O/C ratio, i.e. cellulose content, of 14.70%. Removing spiky shape bodies (Figure 7c) decreases the silica content on the fiber by more than four times (Figure 7a-b). This decrease is due to the removal of lignin from the surface of the fiber, which results in a decrease in the silica bodies binding from the holes (silica cavities). This is consistent with the oil palm empty fruit bunch fiber which showed a similar decrease in silica bodies after the alkaline treatment (Daud, Wahid, and Law 2013).

Figure 7

3.3. FTIR analysis

Figure 8 shows the ATR-FTIR spectra for UEB, UER, TEB3N8h and TER3N4h. The main FTIR bands corresponding to the vibrations of their functional groups are reported in Table 4.

Figure 8 **Table 4**

A broad peak centered at 3338 cm^{-1} is observed and related to hydroxy groups O−H stretching vibration present in cellulose, hemicellulose and lignin. The two sharp peaks at 2919 cm^{-1} and 2852 cm^{-1} are attributed to the asymmetric and symmetric C-H stretching vibration from CH and CH_2 in cellulose and hemicellulose, respectively. The peak at 1735 cm^{-1} is allocated to C=O stretching of the acetyl groups of hemicelluloses. The two peaks at 1646 cm^{-1} and 1597 cm^{-1} are assigned to O-H bending vibrations of water absorbed by cellulose and C=O stretching of carboxylic acid and ester, respectively. The peak at 1508 cm^{-1} confirms the presence of C=C stretching of aromatic skeletal vibration of lignin. The tiny peaks located at 1454 cm^{-1}, 1421 cm^{-1}, 1373 cm^{-1} and 1317 cm^{-1} are attributed to the C-H deformation of lignin, CH_2 symmetric bending from cellulose, bending vibration of C-H and C-O groups of the aromatic ring in polysaccharides, respectively. The peak at 1244 cm^{-1} is allocated to CH stretching of the aromatic skeleton ring vibration of the lignin. The peaks at 1099 cm^{-1} and 1159 cm^{-1} are due to C−O/C−C stretching vibration for ring and the asymmetrical stretching of C−O−C present in cellulose and hemicellulose, respectively. The extensive peak at 1033 cm^{-1} corresponds to C−O stretching modes of hydroxyl and ether groups in cellulose. The smallest peak at 899 cm^{-1} is assignable to β-glycosidic linkages between the monosaccharides. After the alkali treatment, the reduction in intensity or elimination of the transmission bands in the FTIR spectrum for the peaks located at approximately 3338 cm^{-1}, 2852 cm^{-1}, 1735 cm^{-1}, 1373 cm^{-1}, 1244 cm-^{1} can be clearly seen, indicating the removal of lignin and hemicelluloses, the same observations were reported by KılınÇ et al. (KılınÇ et al. 2018) for Tossa/Daisee jute fiber and also by Kasyapi et al. (Kasyapi, Chaudhary, and Bhowmick 2013) for Althea Officinalis L. fiber (Table 4).

3.4. XRD analysis

The X-ray diffraction profiles, crystallinity index, degree of crystallinity and crystallite size for the untreated and treated fibers including the crystal lattice assignments are shown

in Figure 9, respectively, and compared with results reported in the literature for other fibers.

Figure 9

For the untreated fibers, the spectrum exhibits a broad peak at 2θ = 16.19°, a sharp marked peak at 22.14° and a less defined peak at 34.57°. The corresponding crystallographic planes are (110) (200) and (004), respectively, typical of native cellulose. The valley located at 2θ=18.53° corresponds to the amorphous fraction (Iam). For treated fibers, the peaks associated to (110) at 16.19° and the sharp peak associated to (200) at 22.14° were shifted to 15.9° and 22.37°, respectively. Moreover, these peaks become sharper and higher than for the raw fibers, indicating the transformation of the crystal structure of the fiber from cellulose I_α to cellulose I_β after alkali-treatment (Kasyapi, Chaudhary, and Bhowmick 2013). The crystallinity index for UEB, UER, TEB3N8h and TER3N4h was found to be 57.04%, 62.07%, 69.48%, and 67.07%, respectively, while the degree of crystallinity was found to be 69.95%, 72.50%, 76.62 %, and 75.23%, respectively. The maximum values for Cr.I. and Xc were observed for TEB3N8h fiber with an increase of 21.81% and 9.54%, respectively, compared to the untreated fiber, i.e. higher crystallization is associated with a higher tensile strength of the fibers. This increase is due to the removal and reduction of amorphous non-cellulosic compounds, such as impurities, pectin, lignin, and hemicellulose as already observed in FTIR and SEM analysis. Furthermore, the CS value for UEB, UER, TEB3N8h and TER3N4h was found to be 2.83 nm, 2.84 nm, 3.12 nm and 3.09 nm, respectively. The optimization of Cr.I., Xc and CS after alkaline treatment has been found in previous studies for different fibers such as date palm branches (Amroune et al. 2019), Washingtonia palm (Sajid et al. 2019), Mendong grass [31], banana pseudostems (Das et al. 2018), jute fiber (Roy et al. 2012) as shown in Table 5.

Table 4

3.5. TGA analysis

The thermal stability behaviour of raw fibers and those exhibiting the highest tensile strength for the optimal treatment by both extraction methods was analyzed using TGA and DTG (Figure 10).

Figure 10

From room temperature up to 700°C, the curves exhibit four main stages of weight loss. The first stage shows a slight weight loss of approximately 8% from 30°C to 110°C for

both untreated fibers and to 125 °C for treated fibers, due to the water evaporation contained in the fibers. Thereafter, thermal stability up to 235°C was observed for all fibers except TER3N4h, which remains stable up to 220°C. The second stage started from this temperature up to about 300°C and 305°C for the raw and treated fibers, respectively, with an estimated weight loss around 23% and 26%, which corresponds to the decomposition of the hemicelluloses. The third stage for untreated and treated fibers between 300 and 370°C with a weight loss of 39.5% and between 305 and 385°C with a weight loss of around 28%, respectively, is attributed to the degradation of cellulose and partial degradation of lignin. The remarkable difference in weight loss between untreated and treated fibers indicates that the alkali treatment reduced the percentage of lignin in the treated fibers. Finally, the last degradation step occurred in the temperature range 370-475°C for untreated fibers and 385-505°C for treated fibers. The corresponding weight losses were around 24% and 33%, respectively. It is attributed to the degradation of lignin and other non-cellulosic substances (Haddar et al. 2018; Roy et al. 2012). The char content at 700°C was found to be 0.13%, 0.52%, 1.15% and 2.12% for UEB, UER, TEB3N8h and TER3N4h, respectively.

4. CONCLUSIONS

This work investigated the effect of the extraction method and the alkaline treatment parameters on the tensile and physico-chemical properties of Ghars palm rachis fibers. The main conclusions are:

- The analysis of variance revealed that the immersion time is the main factor affecting the tensile properties of the fiber, followed by the NaOH concentration and, finally, the extraction method used;
- Compared to the raw fibers, the optimal treatment led to an improvement of the tensile strength by more than 95% for a NaOH concentration of 3% and an 8-hour immersion time for the fiber extracted by boiling. The regression models showed a good agreement compared to the experimental values with R^2 higher than 98%, which can be used to predict the tensile strength and Young's modulus;
- SEM analysis highlighted that different external fiber surfaces result from the extraction method. The surfaces vary in terms of cleanliness, as well as amount of non-cellulosic materials and impurities adhering to the fiber. However, the alkali treatment cleaned the outer surface by removing or reducing the amount of

impurities, resulting in numerous pores on the fiber surface due to the removal of silica bodies;

- SEM-EDX analysis indicated that the alkali treatment removed a large percentage of hemicelluloses, lignin, wax, and impurities from the surface, resulting in an 14.70% increase in the O/C atomic ratio of cellulose from 0.68 to 0.78;
- The main chemical groups for untreated and treated fibers were identified by ATR-FTIR spectrum analysis and compared to other lignocellulosic fibers reported in the literature;
- The higher Cr.I., Xc, and CS values are associated with the higher tensile strength of the fibers, indicating that crystallinity contributes to improve the tensile properties of the fibers;
- TGA/DTG analysis allowed identifying the degradation temperature for raw and alkali treated fibers components and determining their thermal stability. In addition, it was confirmed that alkali treatments improve the thermal behaviour of the fibers.
- Until now, to the best knowledge of the authors, the only application using the fiber of date palm rachis is the fabrication of particleboards were the used fibers are short and they are obtained by crushing. However, the extraction of these fibers in the long-form shows great potential use and can compete with other natural fibers. Due to their wide availability, low price, and competitive technical properties compared to other natural fibers, it is expected that this fiber will play a major role in many potential applications such as reinforcement of asphalt concrete, gypsum plaster, and cement, also in manufacturing insulating panels. Moreover, it can be used as a reinforcement of polymeric biocomposites in different areas specially in the internal parts of the automotive industry.

References

Abdal-Hay, A., Suardana, N.P.G., Jung, D.Y., Choi, K.S., and Lim, J.K. 2012. Effect of diameters and alkali treatment on the tensile properties of date palm fiber reinforced epoxy composites. *International Journal of Precision Engineering and Manufacturing* 13(7):1199–1206. doi:10.1007/s12541-012-0159-3.

Adekomaya, O. and Majozi, T. 2019. Sustainability of surface treatment of natural fibre in composite formation: challenges of environment-friendly option. *International Journal of Advanced Manufacturing Technology* 105(7–8):3183–3195. doi:10.1007/s00170-019-04581-6.

Agoudjil, B., Benchabane, A., Boudenne, A., Ibos, L., and Fois, M. 2011. Renewable materials to reduce building heat loss: Characterization of date palm wood. *Energy*

and Buildings 43(2–3):491–497. doi:10.1016/j.enbuild.2010.10.014.

Akin, D.E., Slomczynski, D., Rigsby, L.L., and Eriksson, K.-E.L. 2002. Retting Flax with Endopolygalacturonase from Rhizopus oryzae. *Textile Research Journal* 72(1):27–34. doi:10.1177/004051750207200105.

Al-Oqla, F.M., Salit, M.S., Ishak, M.R., and Aziz, N.A. 2015. Selecting natural fibers for bio-based materials with conflicting criteria. *American Journal of Applied Sciences* 12(1):64–71. doi:10.3844/ajassp.2015.64.71.

Amroune, S., Bezazi, A., Belaadi, A., Zhu, C., Scarpa, F., Rahatekar, S., and Imad, A. 2015. Tensile mechanical properties and surface chemical sensitivity of technical fibres from date palm fruit branches (Phoenix dactylifera L.). *Composites Part A: Applied Science and Manufacturing* 71(November):98–106. doi:10.1016/j.compositesa.2014.12.011.

Amroune, S., Bezazi, A., Dufresne, A., Scarpa, F., and Imad, A. 2019. Investigation of the Date Palm Fiber for Green Composites Reinforcement: Thermo-physical and Mechanical Properties of the Fiber. *Journal of Natural Fibers*:1–18. doi:10.1080/15440478.2019.1645791.

Anon n.d. Food and Agriculture Organization Corporate Statistical Database (FAOSTAT) [electronic resource]. http://www.fao.org/faostat/fr/?#data/QC.

Assarar, M., Scida, D., Zouari, W., Saidane, E.H., and Ayad, R. 2016. Acoustic emission characterization of damage in short hemp-fiber-reinforced polypropylene composites. *Polymer Composites* 37(4):1101–1112. doi:10.1002/pc.23272.

Bezazi, A., Belaadi, A., Bourchak, M., Scarpa, F., and Boba, K. 2014. Novel extraction techniques, chemical and mechanical characterisation of Agave americana L. natural fibres. *Composites Part B: Engineering* 66:194–203. doi:10.1016/j.compositesb.2014.05.014.

Boumediri, H., Bezazi, A., Del Pino, G.G., Haddad, A., Scarpa, F., and Dufresne, A. 2019. Extraction and characterization of vascular bundle and fiber strand from date palm rachis as potential bio-reinforcement in composite. *Carbohydrate Polymers* 222. doi:10.1016/j.carbpol.2019.114997.

Cheour, K., Assarar, M., Scida, D., Ayad, R., and Gong, X.L. 2016. Effect of water ageing on the mechanical and damping properties of flax-fibre reinforced composite materials. *Composite Structures* 152:259–266. doi:10.1016/j.compstruct.2016.05.045.

Chonsakorn, S., Srivorradatpaisan, S., and Mongkholrattanasit, R. 2019. Effects of different extraction methods on some properties of water hyacinth fiber. *Journal of Natural Fibers* 16(7):1015–1025. doi:10.1080/15440478.2018.1448316.

Das, B., Chakrabarti, K., Tripathi, S., and Chakraborty, A. 2014. Review of Some Factors Influencing Jute Fiber Quality. *Journal of Natural Fibers* 11(3):268–281. doi:10.1080/15440478.2014.880103.

Das, D., Hussain, S., Kumar Ghosh, A., and Kumar Pal, A. 2018. Studies on cellulose nanocrystals extracted from Musa sapientum: structural and bonding aspects. *Cellulose Chemistry & Technology* 52:729–739.

Daud, W.R.W., Wahid, K.A., and Law, K.N. 2013. Cold soda pulping of oil palm empty fruit bunch (OPEFB). *BioResources* 8(4):6151–6160. doi:10.15376/biores.8.4.6151-6160.

El-abbassi, F.E., Assarar, M., Ayad, R., Bourmaud, A., and Baley, C. 2020. A review on alfa fibre (Stipa tenacissima L .): From the plant architecture to the reinforcement of polymer composites. *Composites Part A* 128(June 2019):105677. doi:10.1016/j.compositesa.2019.105677.

Fatma, N., Allègue, L., Salem, M., Zitoune, R., and Zidi, M. 2019. The effect of doum palm fibers on the mechanical and thermal properties of gypsum mortar. *Journal of Composite Materials* 53(19):2641–2659. doi:10.1177/0021998319838319.

García Del Pino, G., Bezazi, A., Boumediri, H., Kieling, A.C., Silva, C.C., Dehaini, J., Rivera, J.L.V., Valenzuela, M. das G. da S., Díaz, F.R.V., and Panzera, T.H. 2020. Hybrid epoxy composites made from treated curauá fibres and organophilic clay. *Journal of Composite Materials*:002199832094578. doi:10.1177/0021998320945785.

García del Pino, G., Kieling, A.C., Bezazi, A., Boumediri, H., Rolim de Souza, J.F., Valenzuela Díaz, F., Valin Rivera, J.L., Dehaini, J., and Panzera, T.H. 2020. Hybrid Polyester Composites Reinforced with Curauá Fibres and Nanoclays. *Fibers and Polymers* 21(2):399–406. doi:10.1007/s12221-020-9506-7.

Gholampour, A. and Ozbakkaloglu, T. 2020. A review of natural fiber composites: properties, modification and processing techniques, characterization, applications. *Journal of Materials Science* 55(3):829–892. doi:10.1007/s10853-019-03990-y.

Gündołdu, T.K., Deniz, ¯rem, Çalişkan, G., Şahin, E.S., and Azbar, N. 2016. Experimental design methods for bioengineering applications. *Critical Reviews in Biotechnology* 36(2):368–388. doi:10.3109/07388551.2014.973014.

Haddar, M., Elloumi, A., Koubaa, A., Bradai, C., Migneault, S., and Elhalouani, F. 2018. Synergetic effect of Posidonia oceanica fibres and deinking paper sludge on the thermo-mechanical properties of high density polyethylene composites. *Industrial Crops and Products* 121:26–35. doi:10.1016/j.indcrop.2018.04.075.

Hanana, S., Elloumi, A., Placet, V., Tounsi, H., Belghith, H., and Bradai, C. 2015. An efficient enzymatic-based process for the extraction of high-mechanical properties alfa fibres. *Industrial Crops and Products* 70:190–200. doi:10.1016/j.indcrop.2015.03.018.

Kasyapi, N., Chaudhary, V., and Bhowmick, A.K. 2013. Bionanowhiskers from jute: Preparation and characterization. *Carbohydrate Polymers* 92(2):1116–1123. doi:10.1016/j.carbpol.2012.10.021.

KılınÇ, A.Ç., Köktaş, S., Atagür, M., and Seydibeyoglu, M.Ö. 2018. Effect of Extraction Methods on the Properties of Althea Officinalis L. Fibers. *Journal of Natural Fibers* 15(3):325–336. doi:10.1080/15440478.2017.1325813.

Konczewicz, W., Kryszak, N., Nowaczkiewicz, E., and Kozlowski, R. 2013. Osmosis Phenomena Based Degumming of Bast Fibrous Plants as a Promising Method in Primary Processing. *Molecular Crystals and Liquid Crystals* 571(1):116–131. doi:10.1080/15421406.2012.703912.

Laghouiter, O.K., Benalia, M., Gourine, N., Djeridane, A., Bombarda, I., Yousfi, M., and Kelthoum Laghouiter, O. 2018. Chemical characterization and in vitro antioxidant capacity of nine Algerian date palm cultivars (Phoenix dactylifera L.) seed oil. *Mediterranean Journal of Nutrition and Metabolism* 11(2):103–117. doi:10.3233/MNM-17185.

Liu, M., Silva, D.A.S., Fernando, D., Meyer, A.S., Madsen, B., Daniel, G., and Thygesen, A. 2016. Controlled retting of hemp fibres: Effect of hydrothermal pre-treatment and enzymatic retting on the mechanical properties of unidirectional hemp/epoxy composites. *Composites Part A: Applied Science and Manufacturing* 88:253–262. doi:10.1016/j.compositesa.2016.06.003.

Ma, P., Lan, J., Feng, Y., Liu, R., Qu, J., and He, H. 2016. Effects of continuous steam explosion on the microstructure and properties of eucalyptus fibers. *BioResources* 11(1):1417–1431. doi:10.15376/biores.11.1.1417-1431.

Maache, M., Bezazi, A., Amroune, S., Scarpa, F., and Dufresne, A. 2017. Characterization of a novel natural cellulosic fiber from Juncus effusus L. *Carbohydrate Polymers* 171:163–172. doi:10.1016/j.carbpol.2017.04.096.

Mohanty, J.R., Das, S.N., Das, H.C., and Swain, S.K. 2014. Effect of chemically modified date palm leaf fiber on mechanical, thermal and rheological properties of polyvinylpyrrolidone. *Fibers and Polymers* 15(5):1062–1070. doi:10.1007/s12221-014-1062-6.

Mouhoubi, S., Bourahli, M.E.H., Osmani, H., and Abdeslam, S. 2017. Effect of Alkali Treatment on Alfa Fibers Behavior. *Journal of Natural Fibers* 14(2):239–249. doi:10.1080/15440478.2016.1193088.

Mumthas, A.C.S.I., Wickramasinghe, G.L.D., and Gunasekera, U.S. 2019. Effect of physical, chemical and biological extraction methods on the physical behaviour of banana pseudo-stem fibres: Based on fibres extracted from five common Sri Lankan cultivars. *Journal of Engineered Fibers and Fabrics* 14:155892501986569. doi:10.1177/1558925019865697.

Nagarajan, V., Mohanty, A.K., and Misra, M. 2013. Sustainable green composites: Value addition to agricultural residues and perennial grasses. *ACS Sustainable Chemistry and Engineering* 1(3):325–333. doi:10.1021/sc300084z.

Pandey, S.N. 2007. Ramie fibre: Part I. Chemical composition and chemical properties. A critical review of recent developments. *Textile Progress* 39(1):1–66. doi:10.1080/00405160701580055.

Prabhakaran, S., Krishnaraj, V., Sharma, S., Senthilkumar, M., Jegathishkumar, R., and Zitoune, R. 2020. Experimental study on thermal and morphological analyses of green composite sandwich made of flax and agglomerated cork. *Journal of Thermal Analysis and Calorimetry* 139(5):3003–3012. doi:10.1007/s10973-019-08691-x.

Prithivirajan, R., Jayabal, S., Sundaram, S.K., and Sangeetha, V. 2016. Hybrid biocomposites from agricultural residues: Mechanical, water absorption and tribological behaviors. *Journal of Polymer Engineering* 36(7):663–671. doi:10.1515/polyeng-2015-0113.

Roy, A., Chakraborty, S., Kundu, S.P., Basak, R.K., Basu Majumder, S., and Adhikari, B. 2012. Improvement in mechanical properties of jute fibres through mild alkali treatment as demonstrated by utilisation of the Weibull distribution model. *Bioresource Technology* 107:222–228. doi:10.1016/j.biortech.2011.11.073.

Saaidia, A., Bezazi, A., Belbeh, A., Bouchelaghem, H., Scarpa, F., and Amirouche, S. 2017. Mechano-physical properties and statistical design of jute yarns. *Measurement: Journal of the International Measurement Confederation* 111:284–

294. doi:10.1016/j.measurement.2017.07.054.

Saba, N., Jawaid, M., Sultan, M.T.H., and Alothman, O.Y. 2017. Green biocomposites for structural applications. *Green Energy and Technology*(9783319493817):1–27. doi:10.1007/978-3-319-49382-4_1.

Sajid, L., Azmami, O., El ahmadi, Z., Benayada, A., and Gmouh, S. 2019. Extraction and characterization of palm fibers and their use to produce wool- and polyester-blended nonwovens. *Journal of Industrial Textiles*:152808371987700. doi:10.1177/1528083719877007.

Sanjay, M.R., Siengchin, S., Parameswaranpillai, J., Jawaid, M., Pruncu, C.I., and Khan, A. 2019. A comprehensive review of techniques for natural fibers as reinforcement in composites: Preparation, processing and characterization. *Carbohydrate Polymers* 207:108–121. doi:10.1016/j.carbpol.2018.11.083.

Siakeng, R., Jawaid, M., Ariffin, H., Sapuan, S.M., Asim, M., and Saba, N. 2019. Natural fiber reinforced polylactic acid composites: A review. *Polymer Composites* 40(2):446–463. doi:10.1002/pc.24747.

Sukudom, N., Jariyasakoolroj, P., Jarupan, L., and Tansin, K. 2019. Mechanical, thermal, and biodegradation behaviors of poly(vinyl alcohol) biocomposite with reinforcement of oil palm frond fiber. *Journal of Material Cycles and Waste Management* 21(1):125–133. doi:10.1007/s10163-018-0773-y.

Suryanto, H., Yudy, E.M., Irawan, S., and Soenoko, R. 2014. Effect of Alkali Treatment on Crystalline Structure of Cellulose Fiber from Mendong (Fimbristylis globulosa) Straw. *Key Engineering Materials.* 594:720–724. doi:www.scientific.net/KEM.594-595.720.

Toubal, L., Zitoune, R., Collombet, F., and Gleizes, N. 2018. Moisture Effects on the Material Properties of a Jute/Epoxy Laminate: Impulse Excitation Technique Contribution. *Journal of Natural Fibers* 15(1):39–52. doi:10.1080/15440478.2017.1302389.

Wei, J. and Meyer, C. 2015. Degradation mechanisms of natural fiber in the matrix of cement composites. *Cement and Concrete Research* 73:1–16. doi:10.1016/j.cemconres.2015.02.019.

Table 1. Factors and levels used in Taguchi design.

Factor	Symbol	Level 1	Level 2	Level 3	Level 4
NaOH concentration (%)	A	1	2	3	5
Treatment time (h)	B	1	4	8	12
Extraction method	C	1	2	-	-

Extraction method: (1) Boiling in water, (2): Retting in water

Table 2. Experimental results detailed for Taguchi L16.

Run	A	B	C	Tensile strength (MPa)	S/N Ratio (dB)	Young's modulus (GPa)	S/N Ratio (dB)	Average diameter (µm)
UEB-raw	-	-	1	116.06 ± 32.70	-	5.64±1.95	-	529 ± 74
UER-raw	-	-	2	103.63 ± 24.88	-	4.38±1.14	-	508 ± 64
1	1	1	1	165.27 ± 78.93	44.36	6.17±1.92	15.80	439 ± 51
2	1	4	1	189.01 ± 90.94	45.53	7.32±2.21	17.29	431 ± 44
3	1	8	2	167.29 ± 50.87	44.47	7.06±1.45	16.97	417 ± 52
4	1	12	2	161.81 ± 24.82	44.18	6.93±1.57	16.81	384 ± 37
5	2	1	1	181.18 ± 88.13	45.16	6.41±2.40	16.14	443 ± 49
6	2	4	1	206.13 ± 96.12	46.28	7.34±2.30	17.31	463 ± 64
7	2	8	2	188.63 ± 65.85	45.51	7.67±2.63	17.70	387 ± 41
8	2	12	2	188.10 ± 88.16	45.49	7.63±2.01	17.65	390 ± 33
9	3	1	2	175.87 ± 54.91	44.90	7.54±2.27	17.55	387 ± 45
10	3	4	2	**192.70 ± 46.58**	45.70	**7.89±1.42**	17.94	375 ± 27
11	3	8	1	**227.04 ± 95.24**	47.65	8.41±2.67	19.01	413 ± 39
12	3	12	1	223.59 ± 80.28	46.99	**8.66±2.66**	18.75	421 ± 56
13	5	1	2	161.36 ± 29.57	44.16	7.33±1.48	17.30	366 ± 57
14	5	4	2	182.36 ± 63.51	45.22	7.73±2.07	17.76	373 ± 39
15	5	8	1	190.61 ± 106.9	45.60	6.65±2.10	16.46	439 ± 57
16	5	12	1	185.37 ± 86.25	45.36	6.99±1.73	16.90	424 ± 51

UEB-raw and UER-raw: Untreated fibers extracted by boiling in water and retting in water, respectively.

Table 3. ANOVA results for tensile strength and Young's modulus.

Source	DF	Tensile strength				Young's modulus			
		Sum of squares	Mean square	F-Value	P-Value	Sum of squares	Mean square	F-Value	P-Value
Model	8	5665.51	708.19	170.80	<0.001	6.573	0.822	81.66	<0.001
A	1	359.18	359.18	86.63	<0.001	0.020	0.020	2.00	0.200
B	1	789.73	789.73	190.47	<0.001	2.112	2.112	209.91	<0.001
C	1	446.28	446.28	107.64	<0.001	0.052	0.052	5.17	0.057
A^2	1	1972.83	1972.83	475.82	<0.001	1.468	1.468	145.93	<0.001
B^2	1	786.22	786.22	189.62	<0.001	0.544	0.544	54.05	<0.001
A×B	1	18.78	18.78	4.53	0.071	0.075	0.075	7.44	0.029
A×C	1	314.85	314.85	75.94	<0.001	1.121	1.121	111.37	<0.001
B×C	1	36.96	36.96	8.91	0.020	0.860	0.860	85.49	<0.001
Error	7	29.02	4.15			0.070	0.010		
Total	15	5694.53				6.644			
Regression		R^2 = 99.94%; Adj-R^2 = 98.91%; Pre-R^2 = 97.16%				R^2 = 98.94%; Adj-R^2= 97.73%; Pre-R^2 = 95.99%			

Table 4. Vibration of the main bands observed in ATR-FTIR spectra for fibers

Vascular fiber of date palm rachis Present work				**Tossa/Daisee jute fiber** (Kasyapi, Chaudhary, and Bhowmick 2013)		**Althea Officinalis L. Fiber** (KılınÇ et al. 2018)		**Vibration**	**Reference**
UEB	**UER**	**TEB3N8h**	**TER3N4h**	**Raw**	**T2N48h**	**Raw**	**T5N2h**		
3338	3340	3334	3347	3336	3335	3300	3300	Hydroxy groups O−H stretching vibration from cellulose, hemicellulose and lignin	(García del Pino et al. 2020)
2919 2852	2917 2848	2921	2918	2915 2853	2901	2920 2850	2920	C−H stretching vibration from CH and CH_2 in cellulose and hemicellulose	(Amroune et al. 2015; Bezazi et al. 2014)
1735	1727	-	-	1738	-	1737	-	C=O stretching of the acetyl groups of hemicelluloses	(Das et al. 2018; Mouhoubi et al. 2017)
1646	1646	1646	1646	1646		1636	1636	O−H of water absorbed by cellulose	(Sajid et al. 2019)
1597	1595	1595	1595	1594	1592	1597	1597	C=O stretching of carboxylic acid and ester	(Amroune et al. 2019)
1508	1506	1504	1504	1505	-	1506	1506	C=C stretching of aromatic skeletal vibration of lignin	(Boumediri et al. 2019)
1454	1452	1454	1458	1456				C-H deformation of lignin	(Das et al. 2018)
1421	1421	1423	1419	1424	1424	1425	1425	CH_2 symmetric bending from cellulose	(Roy et al. 2012)
1373	1373	1363	1373	-	-	1373	1373	Bending vibration of C−H	(Bezazi et al. 2014)
1317	1319	1321	1315	1316	1316	1320	1320	C−O groups of the aromatic ring in polysaccharides	(Maache et al. 2017)
1244	1240	-	-	1242	-	1241	-	CH stretching of the aromatic skeleton ring vibration of the lignin	(Saaidia et al. 2017)
1159	1155	1159	1157	1158	1159	1165	1165	Asymmetrical stretching of C−O−C present in cellulose and hemicellulose	(Das et al. 2018)
1099	1103	1103	1097	1103	1105	1106	1106	C−O/C−C stretching vibration for ring	(Kasyapi, Chaudhary, and Bhowmick 2013)
1033	1033	1034	1028	1030	1029	1030	1030	C−O stretching modes of hydroxyl and ether groups in cellulose	(Maache et al. 2017)
899	899	899	899	896	897	890	890	β-glycosidic linkages between the monosaccharides	(Bezazi et al. 2014)

Table 5. Crystalline properties for the raw and alkali treated fibers.

Type of fiber	2θ (°)			Crystalline index (%)	Degree of crystallinity (%)	Crystallite size (nm)	Reference
	110	Amorphous	002				
UEB	16.19	18.40	22.14	57.04	69.95	2.83	Present work
UER	16.19	18.59	22.14	62.07	72.50	2.84	
TEB3N8h	15.99	18.32	22.27	**69.48**	**76.62**	**3.12**	
TER3N4h	15.99	18.39	22.27	67.07	75.23	3.09	
Date palm fruit branches Raw	16.35	≈18.9	22.17	50.47	-	2.98	(Amroune et al. 2019)
Date palm fruit branches 3%NaOH-2h	15.98	≈18.9	22.28	53.89	-	3.36	
Washingtonia palm Raw	16.77	≈18.1	21.53	23	56.45	-	(Sajid et al. 2019)
Washingtonia palm 0.7%NaOH-1.5h	16.38	≈18.6	22.43	55	69.01	-	
Mendong Grass Raw	16.5	18.2	22.1	58.6	70.7	14.67	(Suryanto et al. 2014)
Mendong Grass 7.5%NaOH-2h	16.1	18.2	22.5	67.3	75.4	8.45	
Banana pseudo-stems Raw	14.8	≈19.5	22.5	52.24	-	2.51	(Das et al. 2018)
Banana pseudo-stems 2%NaOH-1h	14.9	≈19.5	22.5	62.94	-	3.22	
Jute fiber Raw	15.62	≈18.5	23.36	50.4	-	2.78	(Roy et al. 2012)
Jute fiber 0.5%NaOH-24h	15.67	≈18.5	22.35	62.6	-	3.43	
Sisal fiber	16.81	≈18.5	22.31	71.2	77.6	3.37	(Wei and Meyer 2015)

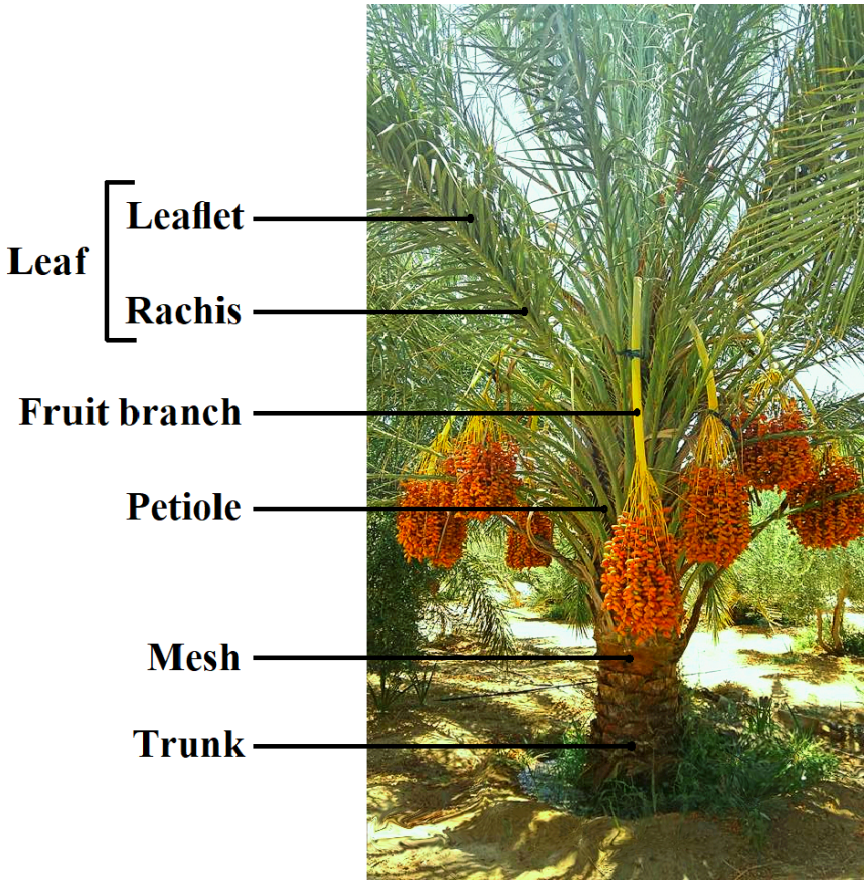

Figure 1. Different components of the date palm tree.

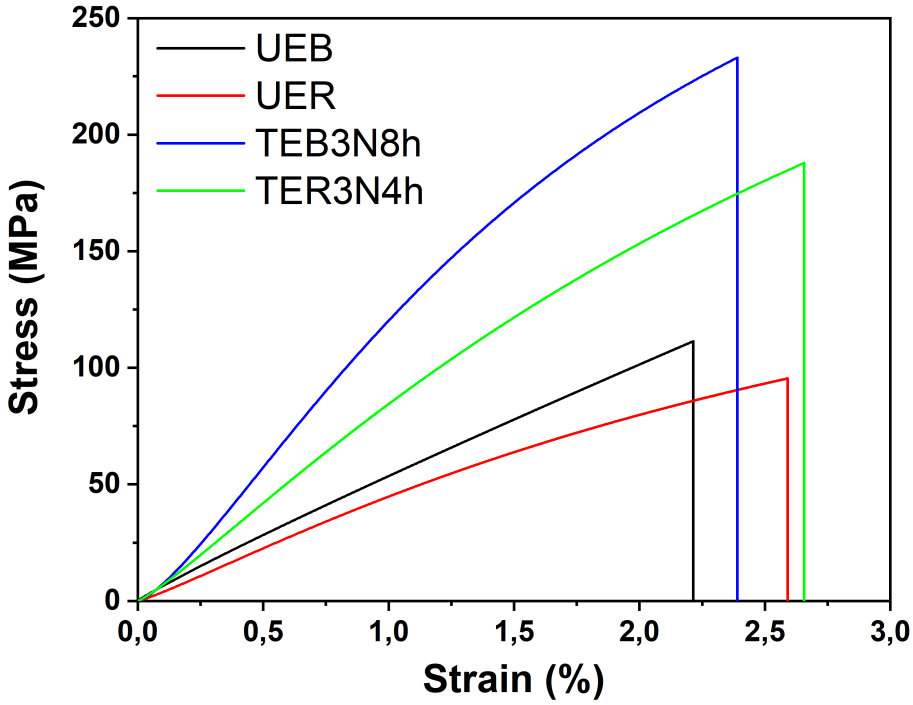

Figure 2. Typical stress–strain curve for UEB, UER, TEB3N8h and TER3N4h.

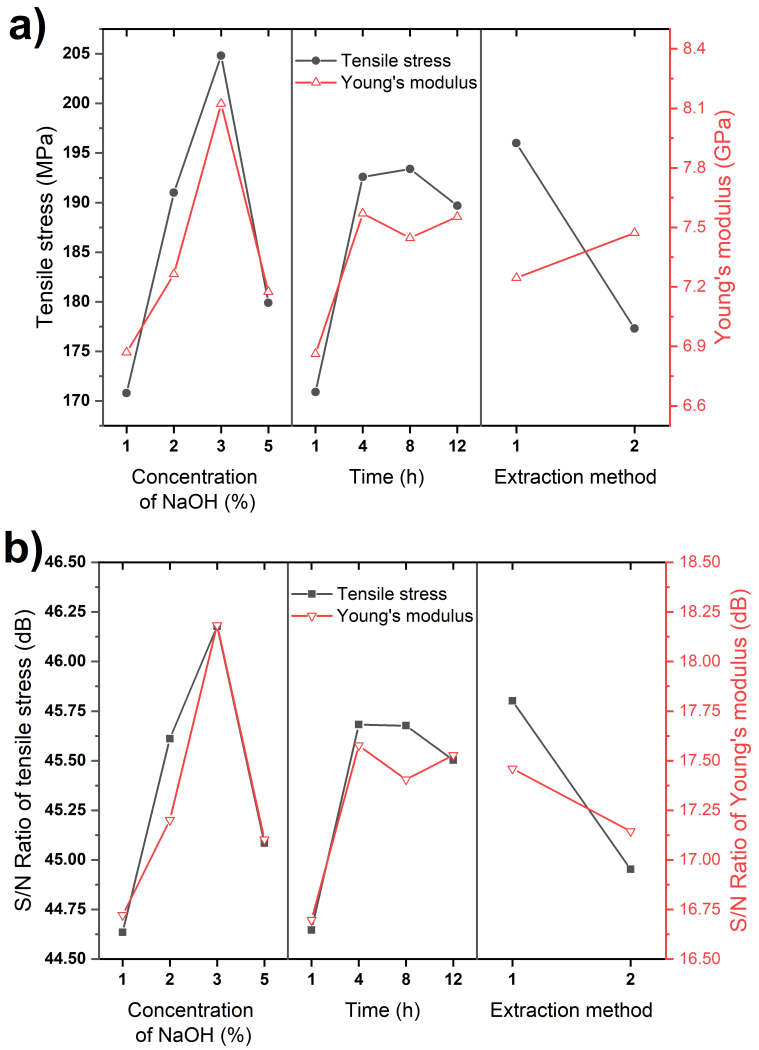

Figure 3. Taguchi design result for TS and E, main effect plot for: a) Means and b) S/N ratio.

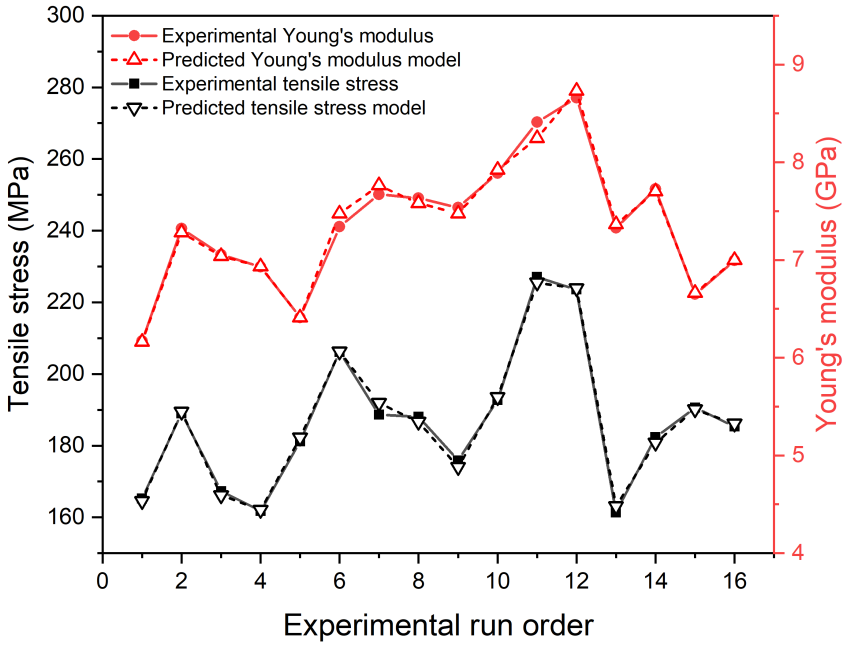

Figure 4. Comparison between experimental data for TS and E with their predicted results.

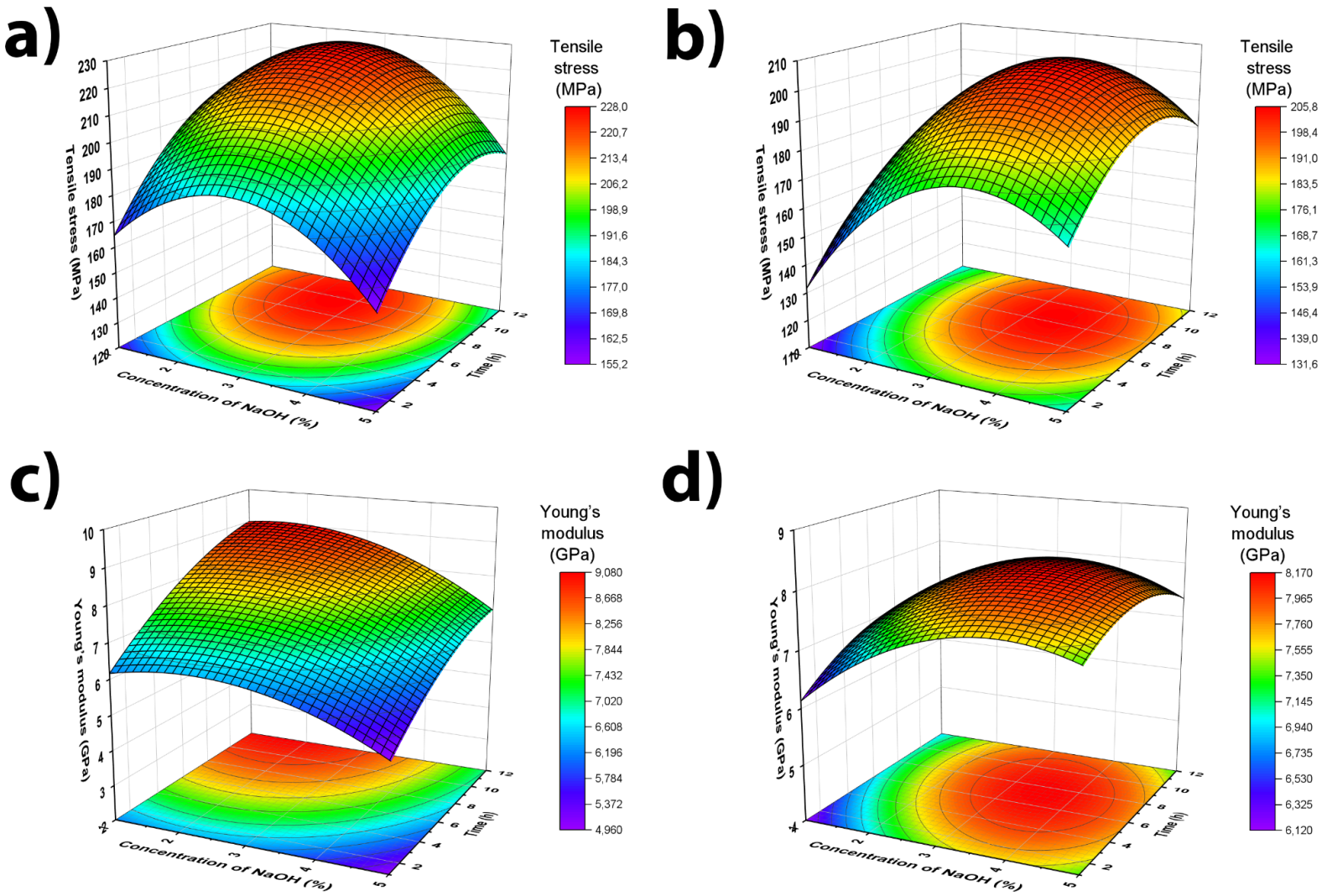

Figure 5. 3D response surface and 2D contour plots showing the effect of the NaOH concentration and immersion time on: (a,b) TS for boiling and retting extraction method, (c,d) E for boiling and retting extraction method.

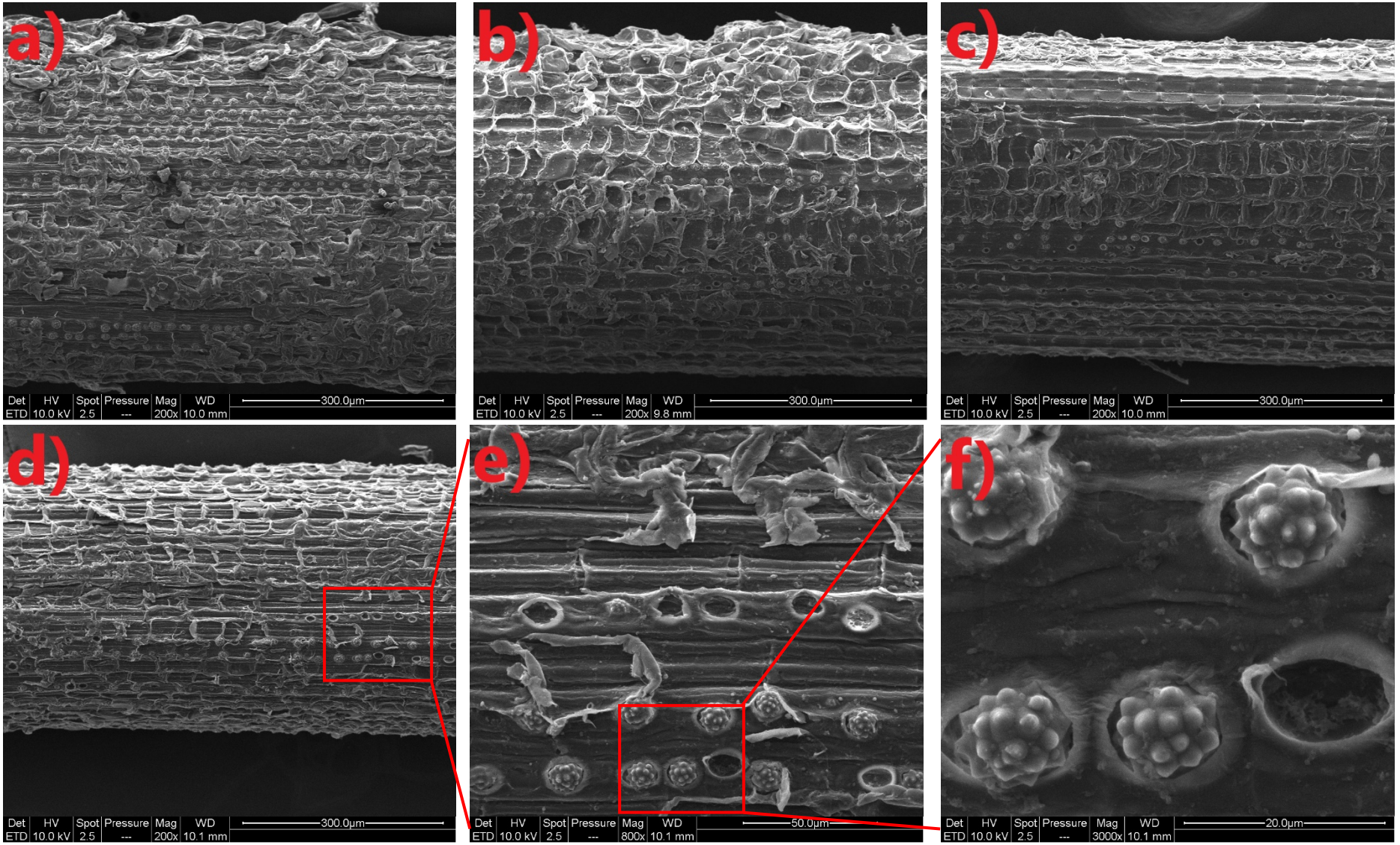

Figure 6. SEM micrographs of the longitudinal surface for: a) UEB, b) UER, c) TEB3N8h, d) TER3N4h, (e,f) Silica bodies and silica cavities with magnification of: x800 and x3000

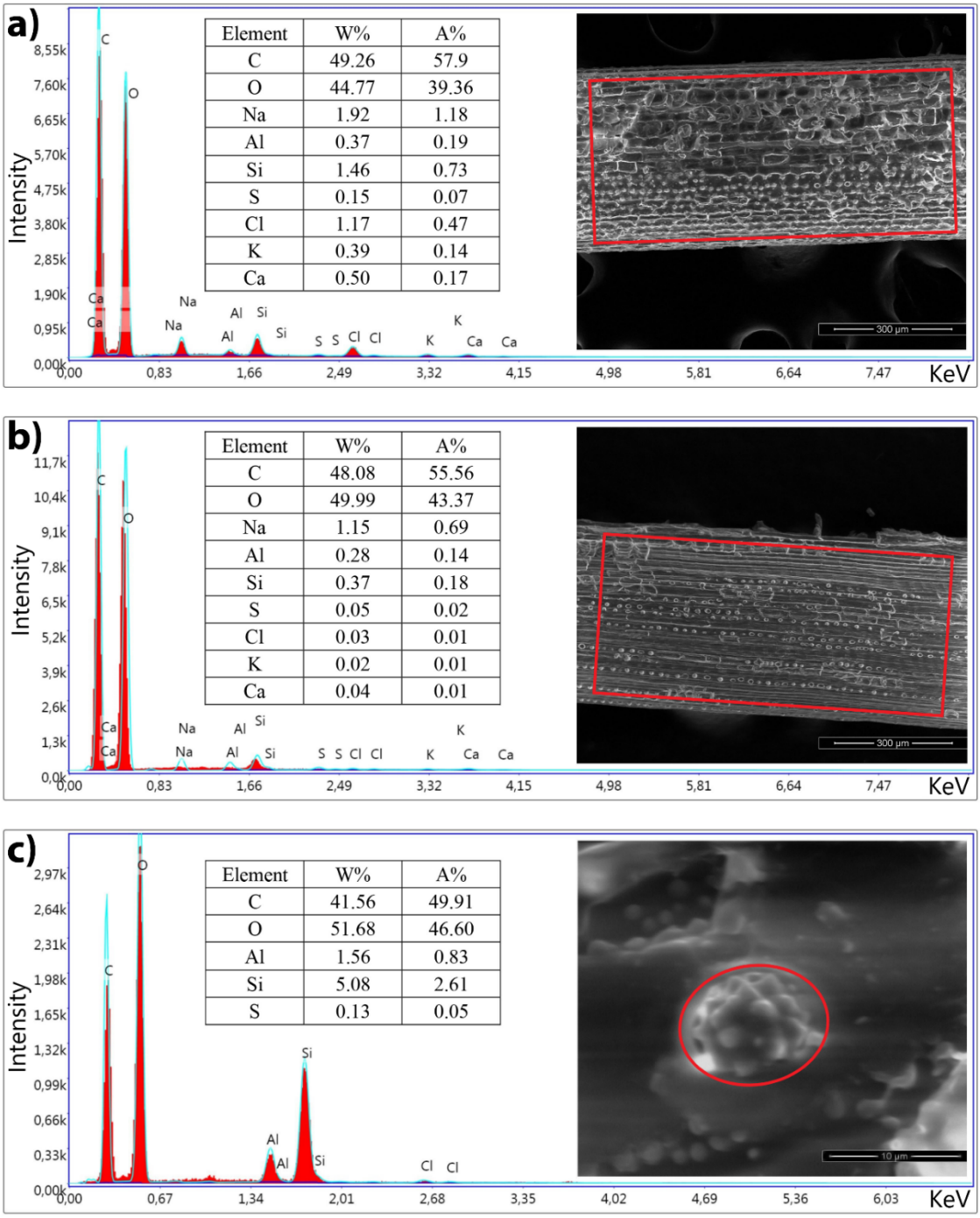

Figure 7. EDX analysis for: a) UEB; b) TEB3N8h, c) silica bodies in UEB.

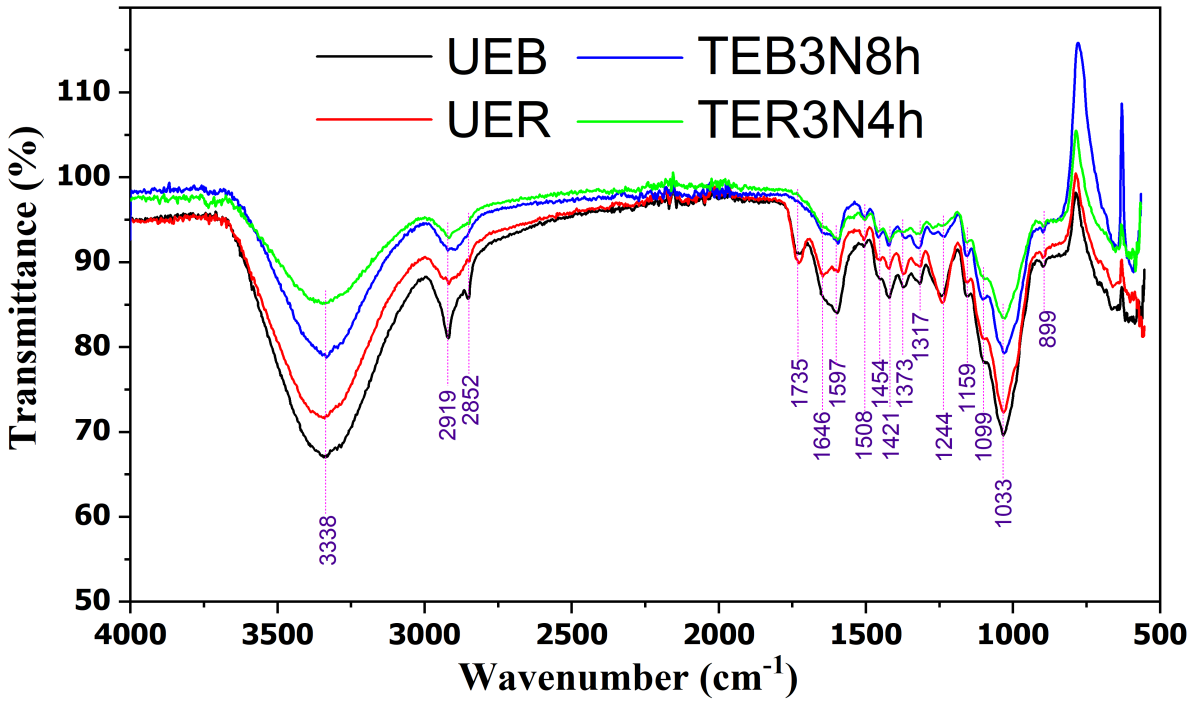

Figure 8. ATR-FTIR for UEB, UER, TEB3N8h and TER3N4h.

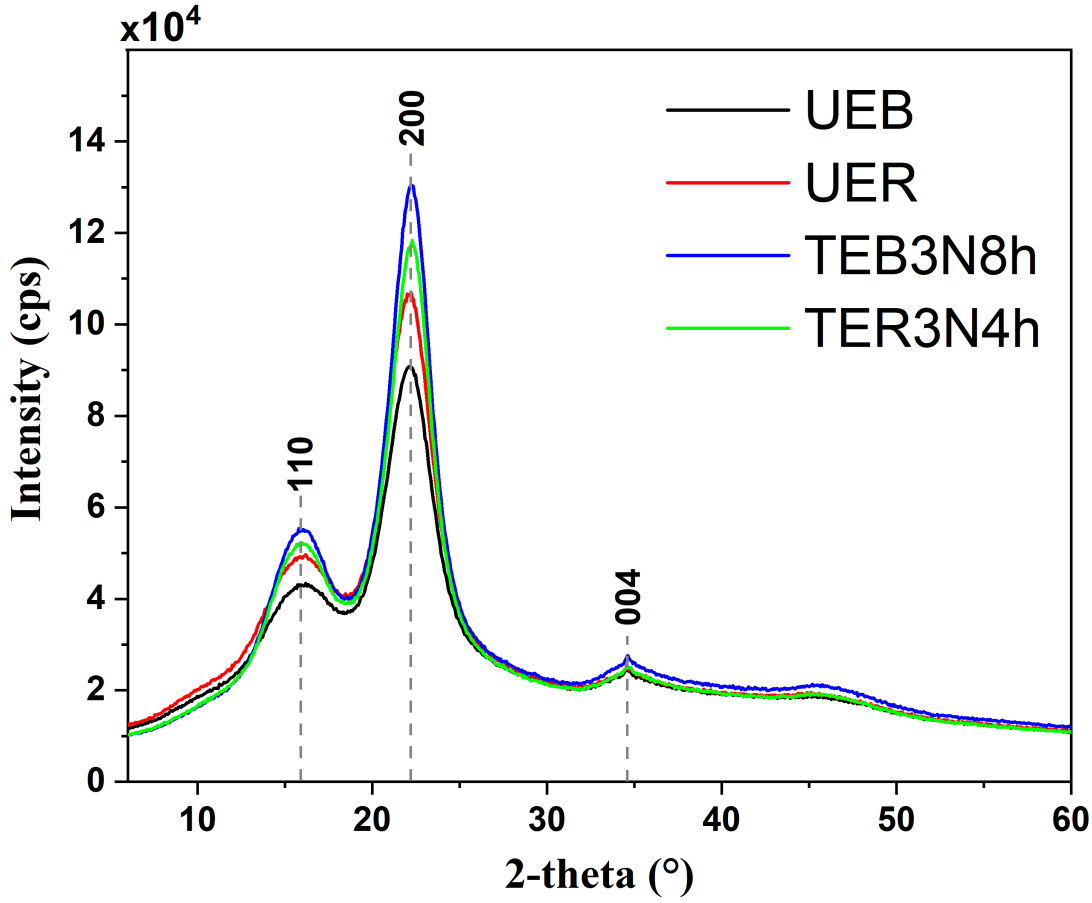

Figure 9. XRD spectra for UEB, UER, TEB3N8h and TER3N4h.

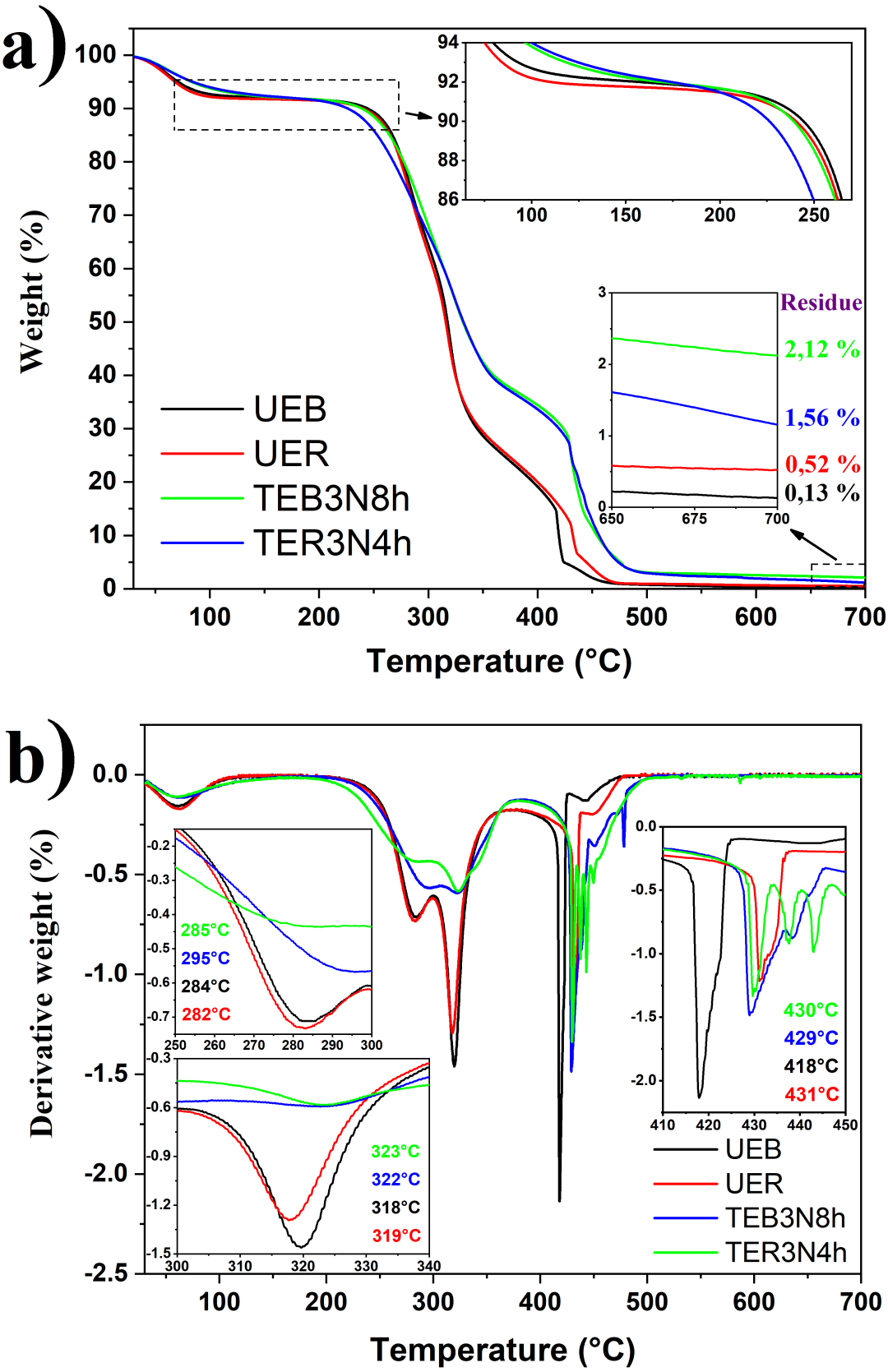

Figure 10. (a) TGA and (b) DTG curves for UEB, UER, TEB3N8h and TER3N4h.